Laboratory Investigation (2019) 99:1428–1441
https://doi.org/10.1038/s41374-019-0267-0

ARTICLE

Preferential expression of sialyl 6′-sulfo *N*-acetyllactosamine-capped *O*-glycans on high endothelial venules in human peripheral lymph nodes

Manami Tsutsumiuchi[1,2] · Hitomi Hoshino[1] · Akiya Kogami[1] · Toshiki Tsutsumiuchi[1,3] · Osamu Yokoyama[2] · Tomoya O. Akama[4,5] · Motohiro Kobayashi[1]

Received: 14 January 2019 / Revised: 15 April 2019 / Accepted: 29 April 2019 / Published online: 31 May 2019

Abstract

Lymphocyte "homing", the physiologic trafficking of lymphocytes from the circulation to secondary lymphoid organs, is regulated by sequential adhesive interactions between lymphocytes and endothelial cells that constitute high endothelial venules (HEVs). Initial lymphocyte "rolling" is mediated by relatively weak, transient adhesive interactions between L-selectin expressed on lymphocytes and sulfated mucin-type *O*-glycans expressed on HEVs. Keratan sulfate galactose (Gal)-6-*O*-sulfotransferase (KSGal6ST) catalyzes 6-*O*-sulfation of Gal in keratan sulfate glycosaminoglycan chains but also transfers sulfate to Gal in much shorter glycan chains, such as sialylated *N*-acetyllactosamine (LacNAc)-capped *O*-glycans. In mice, KSGal6ST is reportedly expressed in HEVs and functions in synthesizing 6-sulfo Gal-containing *O*-glycans on HEVs. However, in humans, the presence of 6-sulfo Gal-containing *O*-glycans on HEVs is not reported. Employing the newly developed monoclonal antibody 297-11A, which recognizes non-sialylated terminal 6′-sulfo LacNAc, we demonstrate that sialyl 6′-sulfo (and/or 6,6′-disulfo) LacNAc-capped *O*-glycans are preferentially displayed on HEVs in human peripheral lymph nodes (PLNs) and to a lesser extent in mesenteric LNs (MLNs) but not in Peyer's patches (PPs). We also found that the scaffold protein mucosal addressin cell adhesion molecule 1 (MAdCAM-1), which is expressed on HEVs in PPs and MLNs but not PLNs, was modified by 297-11A-positive sulfated glycans less efficiently than was CD34. Moreover, 297-11A-positive sulfated glycans were also displayed on HEV-like vessels induced in tumor-infiltrating lymphocyte (TIL) aggregates formed in various cancers. These findings collectively indicate that 297-11A-positive sulfated glycans potentially play a role in physiologic lymphocyte homing as well as in lymphocyte recruitment under pathologic conditions.

Introduction

Circulating lymphocytes continuously enter secondary lymphoid organs such as lymph nodes (LNs) and Peyer's patches (PPs) where they encounter foreign antigens via interaction with antigen-presenting cells [1]. Such physiologic lymphocyte trafficking from the circulation to secondary lymphoid organs is termed "homing" [2].

These authors contributed equally: Manami Tsutsumiuchi, Hitomi Hoshino

Supplementary information The online version of this article (https://doi.org/10.1038/s41374-019-0267-0) contains supplementary material, which is available to authorized users.

✉ Tomoya O. Akama
akamat@hirakata.kmu.ac.jp

✉ Motohiro Kobayashi
motokoba@u-fukui.ac.jp

[1] Department of Tumor Pathology, Faculty of Medical Sciences, University of Fukui, Eiheiji, Japan

[2] Department of Urology, Faculty of Medical Sciences, University of Fukui, Eiheiji, Japan

[3] Department of Otorhinolaryngology and Head and Neck Surgery, Faculty of Medical Sciences, University of Fukui, Eiheiji, Japan

[4] Department of Pharmacology, Kansai Medical University, Hirakata, Japan

[5] Tumor Microenvironment Program, Sanford Burnham Medical Research Institute, La Jolla, CA, USA

Lymphocyte homing is exquisitely regulated by multi-step sequential adhesive interactions between circulating lymphocytes and specialized endothelial cells that constitute high endothelial venules (HEVs) [3, 4]. Interactions begin with lymphocyte "rolling" along the luminal surface of HEVs, followed by chemokine-dependent activation, integrin-mediated firm attachment to the endothelium, and transmigration across HEV walls (Fig. 1) [3, 4].

The initial rolling step of lymphocyte homing is mediated by a relatively weak transient adhesive interaction, analogous to that seen in hook-and-loop fasteners (such as Velcro), between the carbohydrate binding protein L-selectin expressed on lymphocytes and peripheral lymph node addressin (PNAd) expressed on endothelial cells that constitute HEVs [3, 4]. PNAd describes a set of glycoproteins, including CD34 [5, 6] and mucosal addressin cell adhesion molecule 1 (MAdCAM-1) [7, 8], decorated with mucin-type *O*-glycans capped with sialyl Lewis X (Le^X) with 6-*O*-sulfation of *N*-acetylglucosamine (GlcNAc), or sialyl 6-sulfo Le^X (Fig. 2) [2]. PNAd is detected by the monoclonal antibody MECA-79, whose epitope has been shown to be 6-sulfo *N*-acetyllactosamine (LacNAc) attached to extended core 1 *O*-glycans, Galβ1→4(sulfo→6)GlcNAcβ1→3Galβ1→3GalNAcα1→Ser/Thr, which overlaps with sialyl 6-sulfo Le^X, Siaα2→3Galβ1→4[Fucα1→3(sulfo→6)]GlcNAcβ1→R, the L-selectin recognition determinant [9, 10]. Although the MECA-79 antibody epitope does not include a fucose (Fuc) residue in sialyl 6-sulfo Le^X moieties, a Fuc residue is critical for recognition by L-selectin. In this context, Homeister et al. [11] demonstrated that abrogation of α1,3-fucosyltransferase 4 (FucT-4) and FucT-7, which are responsible for biosynthesis of sialyl Le^X in HEVs, results in complete loss of lymphocyte homing.

It was previously assumed that sialyl 6′-sulfo Le^X, i.e. sialyl Le^X with 6-*O*-sulfation of galactose (Gal), Siaα2→3(sulfo→6)Galβ1→4(Fucα1→3)GlcNAcβ1→R, was present as a major L-selectin ligand expressed on HEVs [12, 13]. However, subsequent studies revealed that 6-*O*-sulfation of Gal and α1,3-fucosylation of GlcNAc within the same LacNAc unit was mutually exclusive [11, 14–16]. In this context, Kawashima et al. [17] reported that sialyl 6′-sulfo Le^X was not present in *O*-glycans of mouse GlyCAM-1, although 6-sulfo Gal was present as (i) 6′-sulfo LacNAc attached to core 2 arms, sulfo→6Galβ1→4GlcNAcβ1→6(Galβ1→3)GalNAcα1→Ser/Thr and (ii) terminal 6-sulfo Gal attached to core 1 arms, sulfo→6Galβ1→3GalNAcα1→Ser/Thr. These observations suggest that sialyl 6′-sulfo Le^X is not present on HEVs [18].

Keratan sulfate Gal-6-*O*-sulfotransferase (KSGal6ST) catalyzes Gal-6-*O*-sulfation in keratan sulfate glycosaminoglycan chains, which consist of repeating 6-sulfo LacNAc units intermittently modified with Gal-6-*O*-sulfation (Fig. 3) [19]. KSGal6ST also transfers sulfate to Gal in much shorter glycan chains such as α2,3-sialylated LacNAc-capped *O*-glycans [15, 20]. In this context, Patnode et al. [21] demonstrated in mice that KSGal6ST is expressed in endothelial cells that constitute HEVs in peripheral LNs (PLNs) and mesenteric LNs (MLNs), and that KSGal6ST plays a major role in synthesizing 6-sulfo Gal-containing *O*-glycans, namely sialyl 6,6′-disulfo LacNAc, on HEVs. However, in humans, there are as yet no reports demonstrating the presence of 6-sulfo Gal-containing *O*-glycans on HEVs.

Here, employing the newly developed monoclonal antibody 297-11A, which recognizes non-sialylated terminal 6′-sulfo LacNAc structures, we demonstrate that sialyl 6′-sulfo (and/or 6,6′-disulfo) LacNAc-capped *O*-glycans are preferentially displayed on HEVs in human PLNs and to a lesser extent on those in MLNs, but not on those in PPs. These sulfated glycans were also displayed on HEV-like vessels induced in tumor-infiltrating lymphocyte (TIL) aggregates formed in various cancers. Thus, 297-11A-

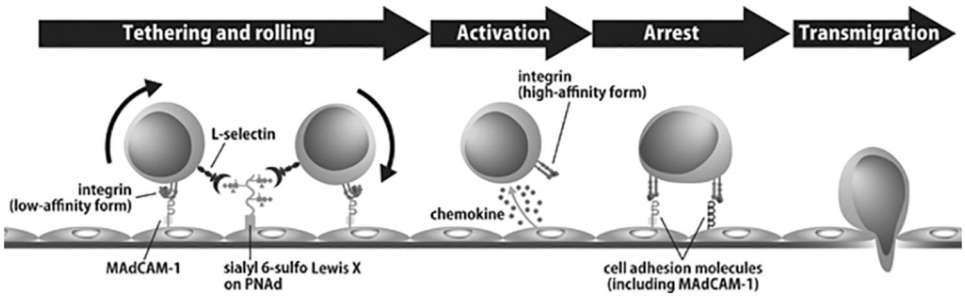

Fig. 1 Schematic representation of sequential adhesive interactions between circulating lymphocytes and high endothelial venules (HEVs) in lymphocyte homing. Shown are four steps: (i) tethering and rolling, mediated by interaction between vascular addressins (sialyl 6-sulfo Lewis X (Le^X), the carbohydrate moiety of peripheral lymph node addressin (PNAd), and mucosal addressin cell adhesion molecule 1 (MAdCAM-1)) and lymphocyte homing receptors (L-selectin and integrins in low-affinity form); (ii) lymphocyte activation by chemokines, which result in a conformational change of integrins to a high-affinity form; (iii) arrest, marked by firm attachment of lymphocytes to HEVs and mediated by integrins in high-affinity form and cell adhesion molecules; and (iv) lymphocyte transmigration across HEV walls. Adapted with permission from ref. [4], © John Wiley and Sons (2015)

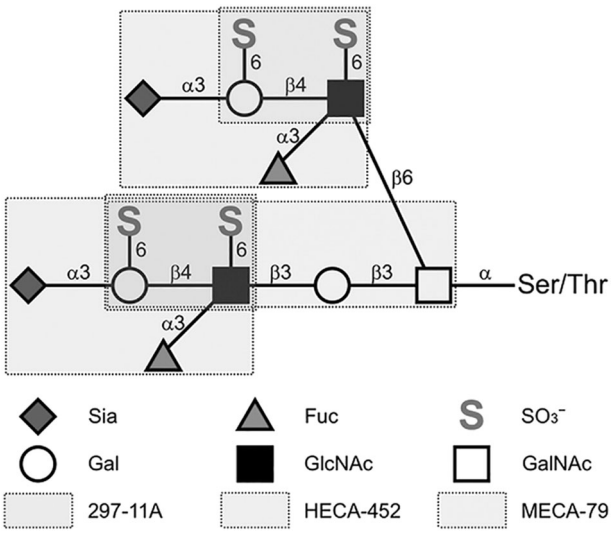

Fig. 2 Carbohydrate structures of sialyl 6,6′-disulfo Le^X attached to both extended core 1 and core 2-branched *O*-glycans, the most fully glycosylated and sulfated putative L-selectin ligands. Epitopes are shown for 297-11A, HECA-452 and MECA-79 monoclonal antibodies. Adapted with permission from ref. [1], © Springer Nature (2012)

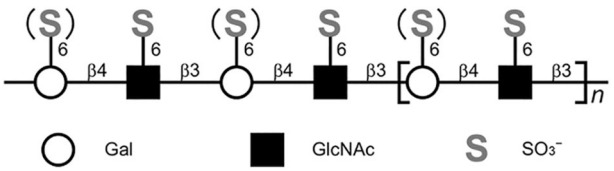

Fig. 3 Carbohydrate structures of keratan sulfate glycosaminoglycan chains. The repeating disaccharide unit (indicated by square brackets) of keratan sulfate is composed of galactose (Gal) and 6-sulfo *N*-acetylglucosamine (GlcNAc) residues, and Gal residues are intermittently 6-*O*-sulfated (indicated by parentheses)

positive sulfated glycans likely function in both physiologic and pathologic lymphocyte trafficking.

Materials and methods

Mice

Chst1 knockout (KO) mice (clone ID: 73827, clone name: 10172A-D6) were obtained from the UC Davis Knock-Out Mouse Project (KOMP) Repository and mated with *Chst5* KO mice [22] to produce *Chst1*/*Chst5* double heterozygous mice, which were then mated once with BALB/c wild type mice and then intercrossed to produce *Chst1*/*Chst5* double KO mice. As double KO mice developed normally with not obvious abnormalities and were fertile, mutant mice were maintained by intercrossing double KO mice. All experimental and maintenance procedures were approved by the Committee for Animal Experiments at Kansai Medical University and conducted according to the Guidelines for Animal Experimentation at Kansai Medical University.

Sulfated glycan-producing cells

cDNAs encoding lumican, β1,3-*N*-acetylglucosaminyltransferase 7 (GlcNAcT-7) and KSGal6ST were amplified from a mouse corneal cDNA library using the polymerase chain reaction (PCR), and each amplicon was cloned into the pCDH lentiviral vector (System Biosciences, Palo Alto, CA). HEK293T cells were then transfected with these vectors plus the psPAX2 helper (Addgene plasmid #12260, a gift from Didier Trono) and pCMV-VSV-G (Addgene plasmid #8454, a gift from Bob Weinberg) vectors. Infectious lentivirus particles secreted from these cells were then used to infect CHO cells or a different batch of HEK293T cells to establish respective CHO-LGK or HEK293T-LGK lines.

Establishment of the monoclonal antibody 297-11A

HEK293T-LGK cells were grown in Dulbecco's modified Eagle's medium (DMEM) containing 10% fetal bovine serum (FBS). 1×10^7 cells were scraped from a 15 cm culture dish and recovered as suspension in a 50 mL conical tube. Cells were then centrifuged at 1000 rpm for 3 min, washed once with phosphate-buffered saline (PBS), and suspended in 1 mL PBS. Two 10-week-old female *Chst1*/*Chst5* double KO mice were then injected intraperitoneally with 500 µL of the cell suspensions and re-immunized in the same manner at 2-week intervals. One week after the third immunization, mice were killed and lymphocytes were collected from the spleen. Of lymphocytes obtained, 5.8×10^6 were mixed with an equal number of SP2/0 mouse myeloma cells, washed three times with electrofusion medium (0.3 M mannitol, 0.1 mM $CaCl_2$, and 0.1 mM $MgCl_2$), suspended in 2.9 mL electrofusion buffer and then subjected to electrofusion using an ECFG21 Super Electro Cell Fusion Generator (Nepa Gene, Chiba, Japan) to generate hybridomas, according to the manufacturer's instructions. After electrofusion, cells were suspended in 60 mL of RPMI 1640 medium containing 8% FBS, 10% BM Condimed H1 Hybridoma Cloning Supplement (Roche Diagnostics, Mannheim, Germany), 55 µM 2-mercaptoethanol, 100 U/mL penicillin and 100 µg/mL streptomycin, seeded into six flat-bottom 96-well plates, and incubated in a CO_2 incubator at 37 °C overnight. Cells were then cultured in selection medium containing 1 × HAT Media Supplement (Sigma-Aldrich, St. Louis, MO) until surviving cells formed colonies. Resulting cell culture medium was assayed by enzyme-linked immunosorbent assay (ELISA) as described below using CHO-LGK cell medium as an antigen solution.

Cells in wells showing strong positive signals by ELISA were cloned by limited dilution. The resulting hybridoma line (designated 297-11A) produced the most robust signals and was expanded and cryopreserved. The monoclonal antibody 297-11A was identified as IgM.

Glycan array analysis

Glycan array analysis using Mammalian Printed Array version 5.1 containing 610 different synthetic glycans was performed at the Consortium for Functional Glycomics (http://www.functionalglycomics.org) as described [23].

Construction of the Siglec-8•IgM expression vector

DNA fragments encoding the Fc region of human IgM were PCR-amplified using the oligonucleotides 5′-CgggATCCg TgATTgCTgAgCTgCCTCCCAA-3′ and 5′-gCTCTAgAT TAgTAgCAggTgCCAgCTgTgT-3′ (respective *Bam*HI and *Xba*I sites underlined) using pcDNA1.1-L-selectin•IgM [24] as a template. Amplicons were digested with *Bam*HI and *Xba*I and inserted into corresponding sites of pcDNA3.1 (Thermo Fisher Scientific, Waltham, MA), resulting in pcDNA3.1-IgM. DNA fragments encoding the extracellular region of human Siglec-8 (amino acid residues 1-358) [25, 26] were also PCR-amplified using the oligonucleotides 5′-CgAAgCTTAAACCCAgACATgCTgCTgC TgCT-3′ and 5′-ACggATCCTTgTgATACAggTCTTgA ggT-3′ (respective *Hind*III and *Bam*HI sites underlined). Template cDNA was prepared from human eosinophil total RNA using SuperScript III reverse transcriptase (Thermo Fisher Scientific), based on the manufacturer's protocols [27]. PCR products were digested with *Hind*III and *Bam*HI and inserted into corresponding sites of pcDNA3.1-IgM, resulting in pcDNA3.1-Siglec-8•IgM.

Siglec-8•IgM chimera binding assay

To obtain Siglec-8•IgM chimeras, COS-1 cells were transiently transfected with pcDNA3.1-Siglec-8•IgM using Lipofectamine Plus (Thermo Fisher Scientific) based on the manufacturer's protocols. Conditioned medium was recovered in 72 h and concentrated ~20-fold using Centriprep YM-30 (Millipore, Billerica, MA). Formalin-fixed, paraffin-embedded (FFPE) sections of HEK293T-LGK cells were incubated with Siglec-8•IgM chimeras in the presence or absence of 5 mM ethylenediaminetetraacetic acid (EDTA) for 60 min. After washing with DMEM, sections were incubated 60 min with Alexa Fluor 488-conjugated anti-human IgM antibody (Thermo Fisher Scientific). After washing, sections were mounted in 50% glycerol/PBS and observed under a fluorescence microscope.

Cell-ELISA

HEK293T-LGK cells were seeded into 96-well culture plates at 2×10^4 cells/well 24 h prior to the assay. Cells were then fixed with 20% neutral-buffered formalin and treated 30 min with 0.3% H_2O_2 in methanol to quench endogenous peroxidase activity. After blocking 15 min with 1% bovine serum albumin (BSA) in Tris-buffered saline (TBS), cells were incubated 60 min with 297-11A. After washing with TBS, cells were incubated 60 min with horseradish peroxidase (HRP)-conjugated anti-mouse IgM antibody (Jackson ImmunoResearch, West Grove, PA), washed, and then treated with 100 µL/well 1-Step ABTS (Thermo Fisher Scientific). Absorbance was read at 405 nm against a reference wavelength of 490 nm using a Spectra Max M5 microplate reader with SoftMax Pro software (Molecular Devices, Sunnyvale, CA).

Human tissue samples

FFPE tissue blocks of surgically removed PLNs ($n = 74$) and MLNs ($n = 142$) without cancer metastasis were retrieved from the pathology archives of University of Fukui Hospital. Blocks of cancer-free ileocecal regions rich in PPs, as well as those of chronic cystitis, invasive and non-invasive bladder urothelial carcinomas and colonic and gastric adenocarcinomas, were also retrieved. Analysis of human tissues was approved by the Ethics Committee of the Faculty of Medical Sciences, University of Fukui.

Deglycosylation treatments

Sialic acid in tissue sections was removed by soaking sections in 0.05 N HCl at 70 °C for 60 min (mild acid hydrolysis) [28]. *N*-glycans were removed by incubating sections 60 min with 5000 U/mL peptide *N*-glycanase F (PNGase F) (New England BioLabs, Ipswich, MA) at 37 °C [29].

Immunohistochemistry

In addition to 297-11A, the following monoclonal antibodies were used: QBEND10 (mouse IgG; Immunotech, Marseille, France) directed against human CD34, a marker of vascular endothelial cells [5]; 15-8G-61 (mouse IgG) directed against human MAdCAM-1 [30]; MECA-79 (rat IgM; BD Pharmingen, San Diego, CA) recognizing 6-sulfo LacNAc attached to extended core 1 *O*-glycans (see Fig. 2) [9, 10]; HECA-452 (rat IgM; BD Pharmingen) recognizing sialyl Le^X as well as its sulfated forms (see Fig. 2) [31, 32]; and 5D4 (mouse IgG; Seikagaku, Tokyo, Japan) recognizing linear penta-sulfated hexa-saccharides of poly-LacNAc in glycosaminoglycan chains of keratan sulfate proteoglycans (see Fig. 3) [33]. MECA-79 and HECA-452

immunohistochemistry was carried out using an indirect method as described [23]. Immunohistochemistry for other antibodies was undertaken using the Histofine system (Nichirei, Tokyo, Japan), based on the manufacturer's protocols. Double immunofluorescence staining was conducted essentially as described [34].

HEV quantification

Immunostained slides were scanned with NanoZoomer RS (Hamamatsu Photonics, Hamamatsu, Japan) to obtain whole slide images. The number of vessels positive for respective CD34, MAdCAM-1, MECA-79, HECA-452, and 297-11A antibodies in the entire area of each LN was determined using NDP.view2 Plus software (Hamamatsu Photonics). The number of HEVs positive for MAdCAM-1, MECA-79, HECA-452, and 297-11A antibodies was divided by the number of CD34-positive vessels to calculate the percentage of HEVs positive for each.

Construction of vectors encoding soluble FLAG-tagged CD34 or MAdCAM-1

DNA fragments encoding the extracellular domain of human CD34 (amino acid residues 1–288) or MAdCAM-1 (amino acid residues 1–342) cloned into pCR2.1-TOPO [35] were digested with *Kpn*I/*Bgl*II or *Kpn*I/*Bam*HI, respectively, and inserted into corresponding *Kpn*I/*Bam*HI sites of pcDNA3.1/Hyg-IgG-FLAG, which harbors a FLAG-tagged human IgG Fc region [36], resulting in pcDNA3.1/Hyg-CD34•IgG-FLAG or pcDNA3.1/Hyg-MAdCAM-1•IgG-FLAG, respectively.

Western blot analysis of CD34 and MAdCAM-1

CHO cells stably expressing sialyl 6-sulfo Le^X attached to both extended core 1 and core 2-branched *O*-glycans were previously described [29]. Cells were transiently transfected with pcDNA3-KSGal6ST [37] and either pcDNA3.1/Hyg-CD34•IgG-FLAG, pcDNA3.1/Hyg-MAdCAM-1•IgG-FLAG or pcDNA3.1/Hyg (mock) using Lipofectamine Plus. Conditioned medium was recovered 72 h later, and CD34•IgG-FLAG and MAdCAM-1•IgG-FLAG secreted into the medium were purified using Protein A-Sepharose (Sigma-Aldrich). Western blot analysis was conducted as described [38].

Statistical analysis

Data are reported as means with standard error of the mean (SEM). Differences between groups were statistically analyzed by either paired or unpaired *t*-tests, where appropriate, using GraphPad Prism 7 software (GraphPad Software, La Jolla, CA). P values < 0.05 were considered significant.

Results

297-11A recognizes non-sialylated terminal 6′-sulfo LacNAc

To determine the epitope recognized by the 297-11A monoclonal antibody, we first performed western blot analysis of lysates of CHO cells transfected with cDNA encoding β1,3-*N*-acetylglucosaminyltransferase 7 (GlcNAcT-7), the enzyme catalyzing elongation of sulfated poly-LacNAc, together with cDNA encoding corneal GlcNAc-6-*O*-sulfotransferase (C-GlcNAc6ST, also called GlcNAc6ST-5) [37] and/or KSGal6ST. As shown in Fig. 4a, 297-11A did not react with components of lysates of either CHO-GlcNAcT-7 or CHO-GlcNAcT-7/C-GlcNAc6ST cells, indicating that the antibody does not recognize non-sulfated or 6-sulfo poly-LacNAc. However, the antibody reacted robustly with lysates of both CHO-GlcNAcT-7/KSGal6ST and CHO-GlcNAcT-7/C-GlcNAc6ST/KSGal6ST cells, indicating that it recognizes poly-LacNAc with Gal-6-*O*-sulfation, regardless of GlcNAc-6-*O*-sulfation, namely, 6′-sulfo or 6,6′-disulfo poly-LacNAc.

We then conducted glycan array analysis to evaluate the epitope in greater detail. As shown in Fig. 4b and Supplementary Table 1, 297-11A did not bind to non-sulfated LacNAc (glycan 168) but rather to glycans containing 6′-sulfo LacNAc structures, sulfo→6Galβ1→4GlcNAcβ1→R (glycans 44), regardless of GlcNAc-6-*O*-sulfation (glycan 297) or Galα1,2-fucosylation (glycan 220). The antibody also did not bind to 6′-sulfo LacNAc-containing structures with Galα2,3-sialylation (glycans 46 and 230), Gal-3-*O*-sulfation (glycans 22 and 23) or Gal-4-*O*-sulfation (glycan 39). Thus, we deduce the minimum 297-11A epitope to be non-sialylated terminal 6′-sulfo LacNAc (Fig. 4c, d). Moreover, 297-11A reacts with its GlcNAc-6-*O*-sulfated form, namely non-sialylated terminal 6,6′-disulfo LacNAc. In addition to these type 2 chain-based structures containing Galβ1→4GlcNAcβ1→R, 297-11A also bound to type 1 chains (Galβ1→3GlcNAcβ1→R) with Gal-6-*O*-sulfation (glycans 443), regardless of GlcNAc-6-*O*-sulfation (glycan 444) or Galα1,2-fucosylation (glycan 501). Interestingly, 297-11A bound to 6-sulfo *N*-acetylgalactosamine (GalNAc) attached to GlcNAc in a β1,4-linkage, sulfo→6-GalNAcβ1→4GlcNAcβ1→R (glycan 512), but did not bind to its non-sulfated form (glycan 98).

Importantly, sialyl 6′-sulfo LacNAc structures should be recognized by this antibody following removal of terminal sialic acid. To test this hypothesis, we first confirmed expression of sialyl 6′-sulfo LacNAc on HEK293T cells expressing lumican, GlcNAcT-7 and KSGal6ST (HEK293T-LGK cells) based on Siglec-8•IgM chimera binding, as Siglec-8, which is selectively expressed on

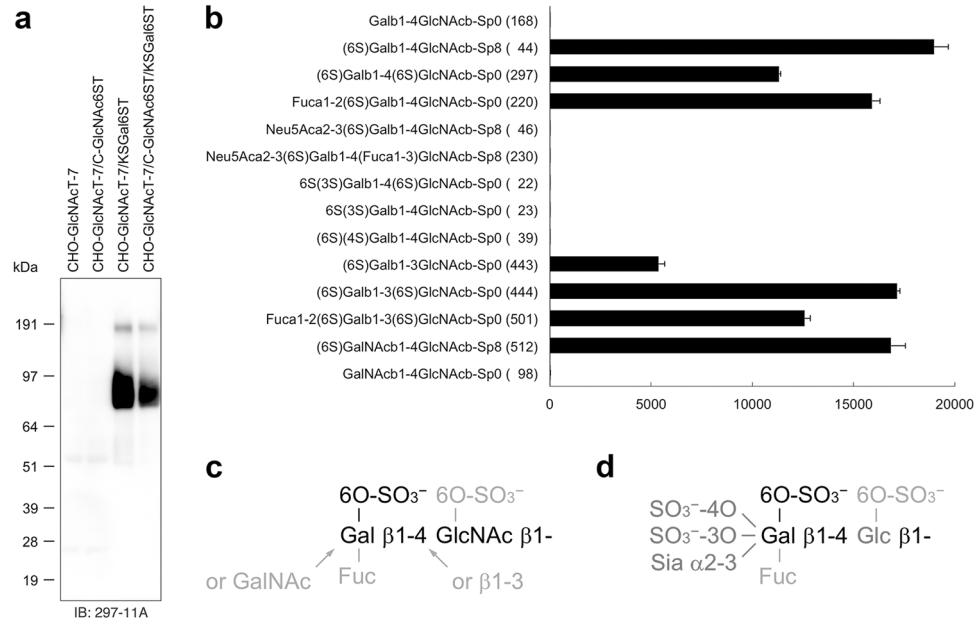

Fig. 4 Determination of 297-11A epitope specificity. **a** Western blot analysis of lysates of CHO cells transfected with cDNAs encoding β1,3-*N*-acetylglucosaminyltransferase 7 (GlcNAcT-7) plus corneal *N*-acetylglucosamine (GlcNAc)-6-*O*-sulfotransferase (C-GlcNAc6ST) and/or keratan sulfate galactose (Gal)-6-*O*-sulfotransferase (KSGal6ST). Membrane was immunoblotted (IB'd) with 297-11A. **b** Glycan array analysis of 297-11A. Screened were a total of 610 different synthetic glycans on Mammalian Printed Array version 5.1, which are listed on the Consortium for Functional Glycomics website (http://www.functionalglycomics.org). Glycan numbers are shown in parentheses after their structures. X-axis represents relative fluorescence units (RFU), and data are presented as means plus SEM of four measurements. Sp0, $CH_2CH_2NH_2$; Sp8, $CH_2CH_2CH_2NH_2$. **c**, **d** Deduced minimum epitope structure (**c**) and modifications that abolish binding (**d**) by the 297-11A antibody. Constituents in black represent the minimum epitope structure, those in red impair antibody binding, and those in gray have no effect

human eosinophils, basophils and mast cells, binds specifically to sialyl 6′-sulfo Le^X and its defucosylated form sialyl 6′-sulfo LacNAc [39, 40]. As shown in Fig. 5a, Siglec-8•IgM chimeras bound to the surface of these cells, an activity abrogated either by calcium ion chelation with EDTA or mild acid hydrolysis to remove terminal sialic acid. We then conducted immunofluorescence staining (Fig. 5b) and cell enzyme-linked immunosorbent assay (ELISA) (Fig. 5c) for 297-11A using the same cells. As expected, both analyses revealed that 297-11A signals were significantly enhanced by mild acid hydrolysis. Overall, these results combined indicate that the 297-11A epitope is non-sialylated terminal 6′-sulfo LacNAc.

Sialyl 6′-sulfo (and/or 6,6′-disulfo) LacNAc-capped *O*-glycans are expressed on HEVs in PLNs and MLNs but not PPs

Sialyl 6,6′-disulfo LacNAc or closely related structures are reportedly expressed on mouse HEVs in PLNs and MLNs but not in PPs [21]. To determine whether similar carbohydrate structures are displayed on human HEVs, we conducted immunohistochemical staining for 297-11A of human PLNs, MLNs and PPs. As shown in Fig. 6, a proportion of MECA-79-positive HEVs in PLNs and MLNs, but not PPs, was also 297-11A-positive, and signal intensity was markedly enhanced after mild acid hydrolysis to remove terminal sialic acid. This finding indicates that these 297-11A-positive HEVs express non-sialylated terminal 6′-sulfo (and/or 6,6′-disulfo) LacNAc as well as sialylated versions of these glycans. Moreover, in acid-treated samples, 297-11A signals were preserved after treatment with peptide *N*-glycanase F (PNGase F). Furthermore, immunostaining of HEVs with 5D4 was negative, indicating that 297-11A signals on HEVs do not originate from glycosaminoglycan chains of keratan sulfate proteoglycans. Overall, these findings indicate that sialyl 6′-sulfo (and/or 6,6′-disulfo) LacNAc-capped mucin-type *O*-glycans are expressed on HEVs in human PLNs and MLNs but not PPs and that most 297-11A signals on HEVs co-localize with those for PNAd, as detected by MECA-79 or HECA-452 (Fig. 7; see also Fig. 2).

297-11A-positive sulfated glycans are preferentially displayed on HEVs in PLNs relative to MLNs

We then conducted quantitative immunohistochemical analysis of HEVs in 216 human LNs consisting of PLNs ($n = 74$) and MLNs ($n = 142$). As shown in Fig. 8a, the

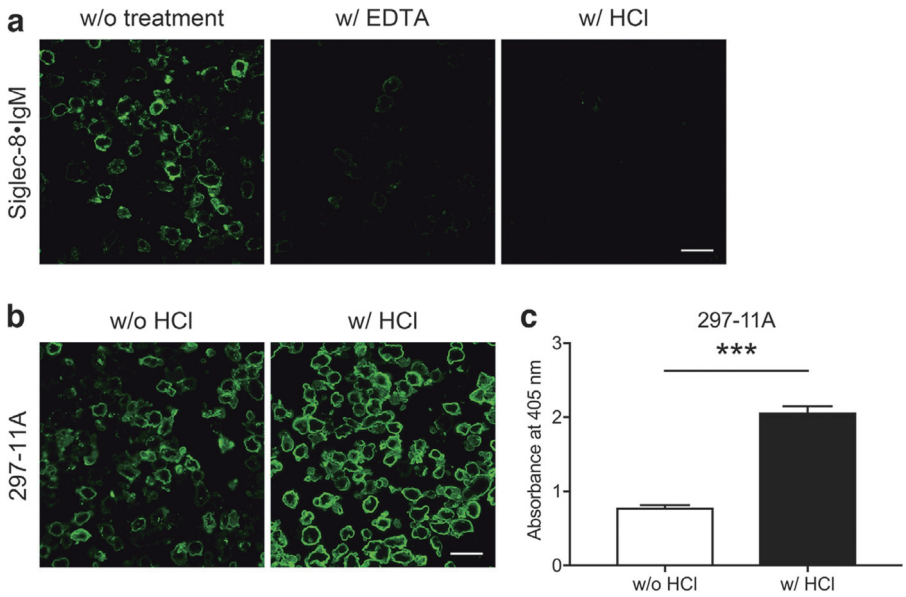

Fig. 5 Monoclonal antibody 297-11A reactivity with sialyl 6′-sulfo *N*-acetyllactosamine (LacNAc) following mild acid hydrolysis to remove terminal sialic acid. **a** Siglec-8•IgM chimera binding to HEK293T cells expressing lumican, β1,3-*N*-acetylglucosaminyltransferase 7 (GlcNAcT-7) and keratan sulfate galactose (Gal)-6-*O*-sulfotransferase (KSGal6ST) (HEK293T-LGK cells) in conditions without (w/o) or with (w/) either ethylenediaminetetraacetic acid (EDTA) or HCl, as indicated. Bar = 20 μm. **b** Immunofluorescence staining for 297-11A using the same cells as in (**a**). Cells were treated with (w/) or without (w/o) HCl. Bar = 20 μm. **c** Cell enzyme-linked immunosorbent assay (ELISA) for 297-11A using the same cells as in (**a**). Cells were treated with (w/) or without (w/o) HCl. Data are presented as means plus SEM of three measurements. ***$P < 0.001$

percentage of MECA-79-positive HEVs among CD34-positive vessels in PLNs (56.9%) was significantly greater than that seen in MLNs (36.8%) ($P < 0.001$). Similarly, the percentage of HECA-452-positive HEVs in PLNs (38.7%) was significantly greater than that seen in MLNs (25.4%) ($P = 0.007$) (Fig. 8b). On the other hand, while 6.9% and 0.9% of vessels in respective PLNs (Fig. 8c) and MLNs (Fig. 8d) were 297-11A-positive, after mild acid hydrolysis those percentages increased significantly to 18.0% and 7.0%, respectively (both $P < 0.001$). This finding indicates that a fraction of HEVs express detectable levels of non-sialylated terminal 6′-sulfo (and/or 6,6′-disulfo) LacNAc-capped *O*-glycans, but a larger proportion of HEVs primarily display sialylated versions of these *O*-glycans. It is noteworthy that, with or without mild acid hydrolysis, the percentage of 297-11A-positive HEVs in PLNs was significantly greater than that seen in MLNs (both $P < 0.001$) (Fig. 8e, f).

CD34 is decorated more highly with 297-11A-positive sulfated glycans than is MAdCAM-1

The paucity of 297-11A-positive HEVs in PPs and MLNs prompted us to ask whether MAdCAM-1, a scaffold protein preferentially expressed on HEVs in PPs and MLNs relative to PLNs [7, 8] (Fig. 9a, b), cannot be modified by the sulfated glycans recognized by 297-11A. To test this hypothesis, we first conducted double immunofluorescence staining of human MLNs for 297-11A and either CD34 or MAdCAM-1 proteins. In support of our hypothesis, 297-11A signals on HEVs co-localize with signals for CD34 rather than those for MAdCAM-1 (Fig. 9c). We then performed immunoblotting for recombinant soluble CD34 and MAdCAM-1 proteins secreted from CHO cells expressing glycosyltransferases and sulfotransferases (including KSGal6ST) required to synthesize the most fully glycosylated and sulfated putative L-selectin ligands (see Fig. 2). As shown in Fig. 9d, while both recombinant proteins were decorated with 297-11A-positive sulfated glycans, CD34 proteins were more heavily decorated with these glycans than were MAdCAM-1 proteins.

HEV-like vessels in lymphoid stroma of various cancers display 297-11A sulfated glycans

To evaluate expression of 297-11A-positive sulfated glycans in pathological settings, we carried out 297-11A immunostaining of various cancers invaded by TILs, since HEV-like vessels are reportedly induced in TIL aggregates

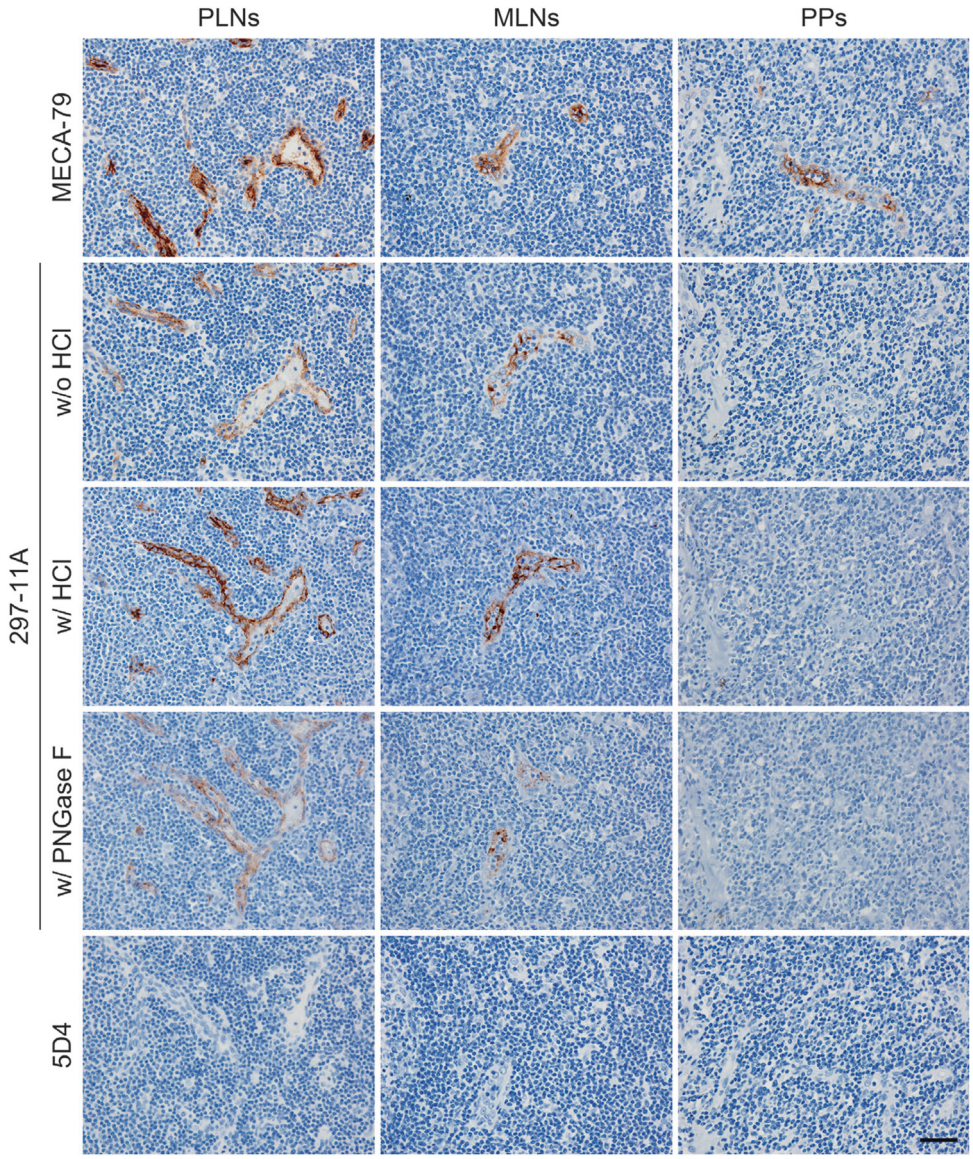

Fig. 6 Immunohistochemical profiles of high endothelial venules (HEVs) in human peripheral lymph nodes (PLNs), mesenteric LNs (MLNs) and Peyer's patches (PPs). Serial sections of indicated tissues were immunostained for MECA-79, 297-11A or 5D4. For 297-11A staining, sections were treated with (w/) or without (w/o) HCl, and HCl-treated sections were further treated with peptide *N*-glycanase F (PNGase F). Signals were visualized with 3,3′-diaminobenzidine (brown), and tissues were counterstained with hematoxylin. Bar = 40 μm

[41]. As shown in Fig. 10, HEV-like vessels induced in TIL aggregates found in invasive and non-invasive bladder urothelial carcinomas and colonic and gastric adenocarcinomas expressed 297-11A-positive sulfated glycans. In addition, 297-11A sulfated glycans were also displayed on HEV-like vessels induced in a chronic inflammatory condition of the bladder, namely chronic cystitis.

Discussion

Employing the newly developed monoclonal antibody 297-11A, we demonstrate that in humans *O*-glycans capped with sialyl 6′-sulfo (and/or 6,6′-disulfo) LacNAc are preferentially displayed on HEVs in PLNs and to a lesser extent on those in MLNs, but not on those in PPs. 297-11A-positive sulfated glycans were also displayed on HEV-like vessels induced in TIL aggregates formed in various cancers. These findings collectively indicate that 297-11A sulfated glycans likely play a role in both physiologic and pathologic lymphocyte trafficking.

In our glycan array analysis, besides type 2 chains (Galβ1→4GlcNAcβ1→R) with Gal-6-*O*-sulfation, 297-11A also bound to type 1 chains (Galβ1→3GlcNAcβ1→R) with Gal-6-*O*-sulfation. A similar phenomenon has been reported following staining with the monoclonal antibody HECA-452, which binds to both sialyl Le^X, Siaα2→3Galβ1→4(Fucα1→3)GlcNAcβ1→R, and sialyl Lewis a (Le^a), Siaα2→3Galβ1→3(Fucα1→4)GlcNAcβ1→R [42]. These two tetra-saccharides have the same sugar composition but

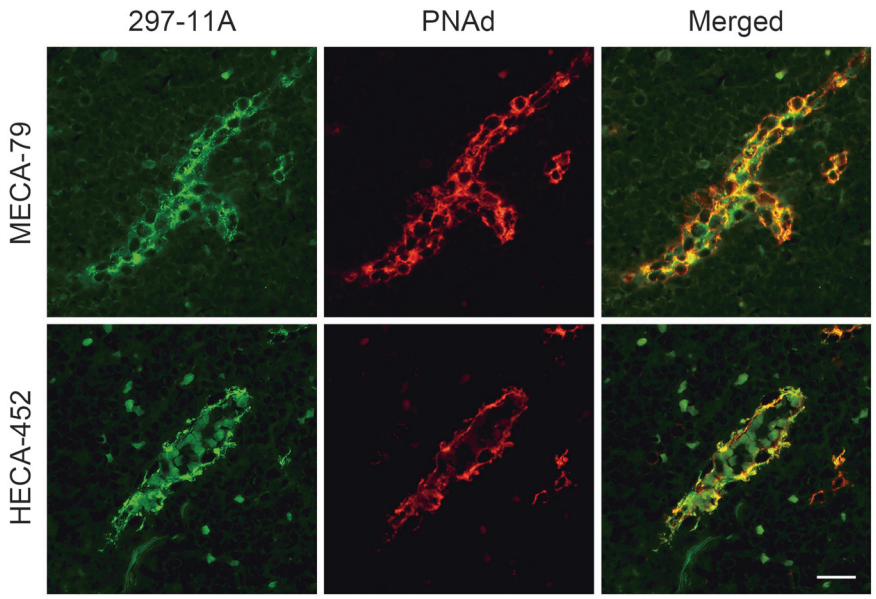

Fig. 7 Double immunofluorescence of HEVs for 297-11A (green) and peripheral lymph node addressin (PNAd) (red), the latter detected by MECA-79 (upper panels) or HECA-452 (lower panels). Yellow signals in merged images indicate co-localization of the two carbohydrate antigens. Bar = 20 μm

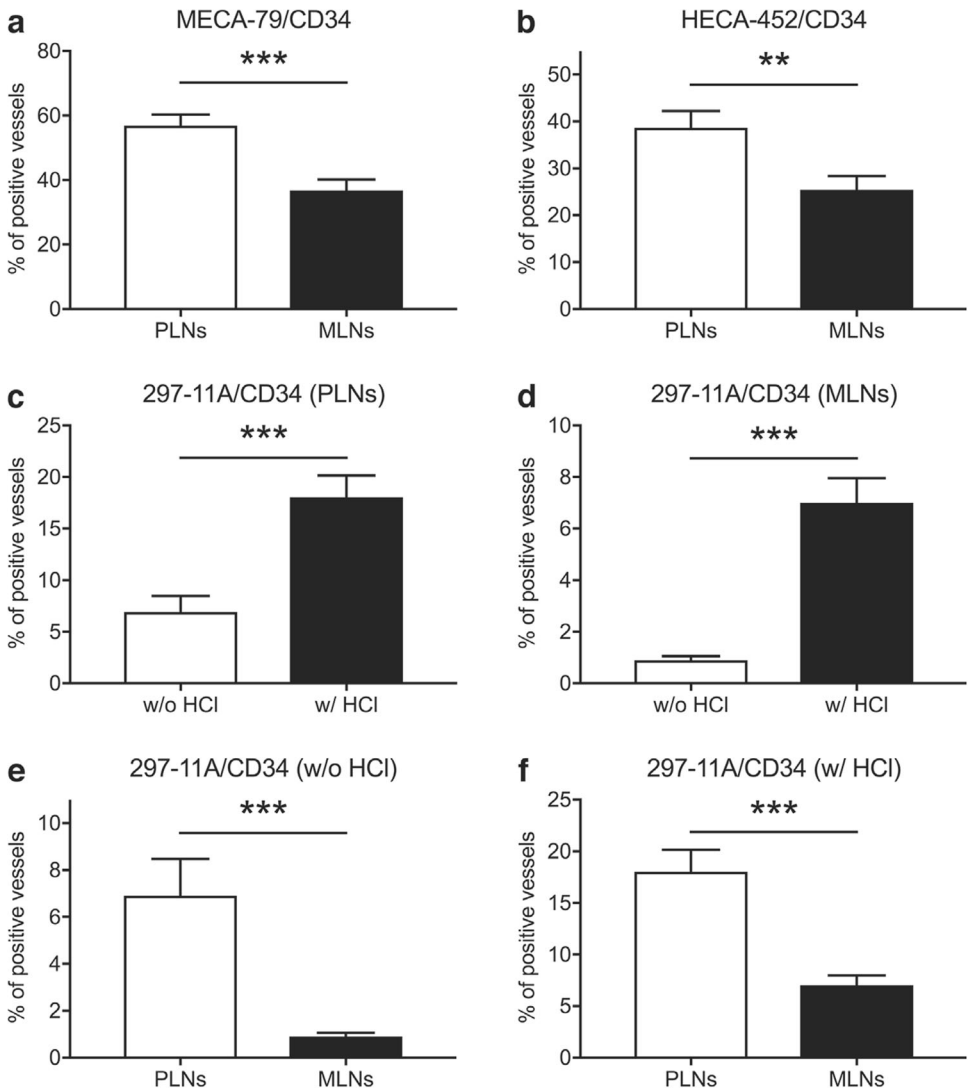

Fig. 8 Quantitative immunohistochemical analysis of high endothelial venules (HEVs) in human peripheral lymph nodes (PLNs) and mesenteric LNs (MLNs). **a**, **b** Percentages of MECA-79-positive (**a**) and HECA-452-positive (**b**) HEVs among CD34-positive vessels in PLNs and MLNs. **c**, **d** Changes in percentages of 297-11A-positive HEVs before (w/o) and after (w/) HCl treatment in PLNs (**c**) and MLNs (**d**). **e**, **f** Percentages of 297-11A-positive HEVs among CD34-positive vessels in PLNs and MLNs without (w/o; **e**) or with (w/; **f**) HCl treatment. Data are presented as means plus SEM. $^{**}P < 0.01$, $^{***}P < 0.001$

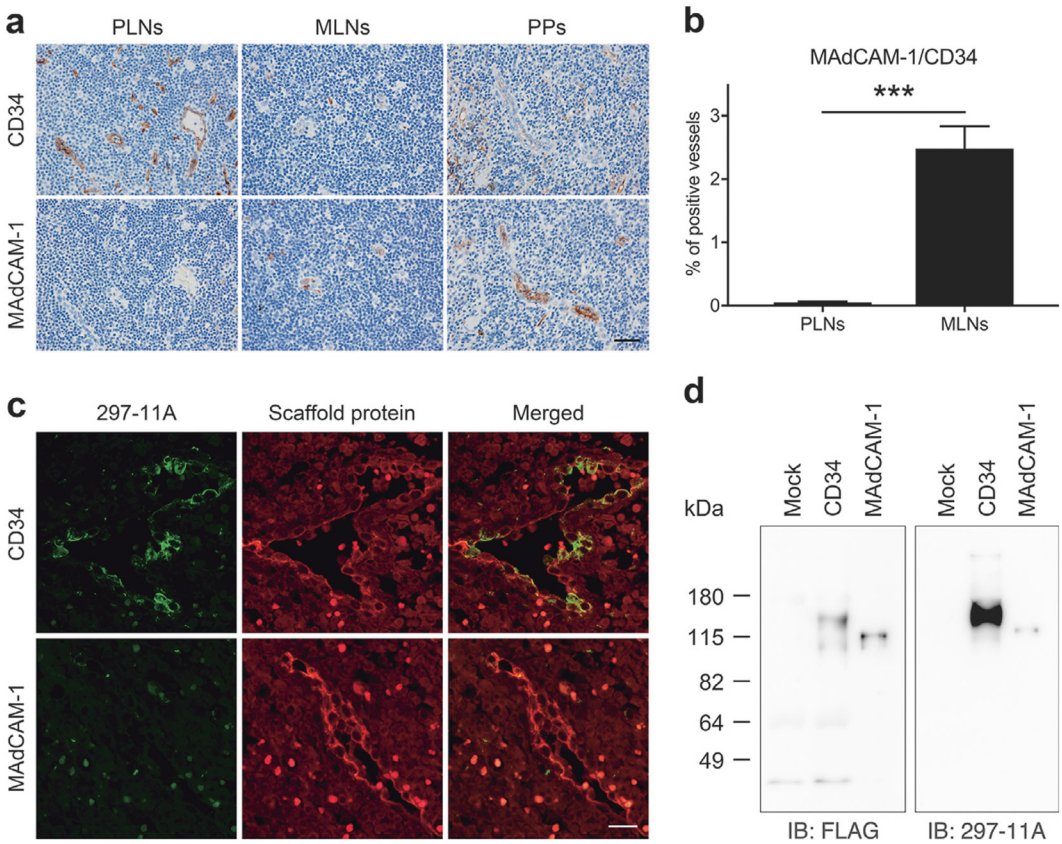

Fig. 9 Preferential decoration of CD34 proteins with 297-11A-positive sulfated glycans as compared to mucosal addressin cell adhesion molecule 1 (MAdCAM-1) proteins. **a** MAdCAM-1 is expressed preferentially on high endothelial venules (HEVs) in Peyer's patches (PPs) and to a lesser extent in mesenteric lymph nodes (MLNs) but is not expressed in peripheral LNs (PLNs). For this analysis, the same tissue sections used in Fig. 6 were subjected to immunostaining for CD34 (upper panels) or MAdCAM-1 (lower panels). Signals were visualized with 3,3′-diaminobenzidine (brown), and tissues were counterstained with hematoxylin. Bar = 40 µm. **b** Quantitative immunohistochemical analysis of a total of 216 human LNs showing the percentage of MAdCAM-1-positive HEVs in PLNs ($n = 74$) and MLNs ($n = 142$). Data are presented as means plus SEM. ***$P <$ 0.001. **c** Double immunofluorescence of MLNs for 297-11A (green) and indicated scaffold proteins (red), namely CD34 (upper panels) or MAdCAM-1 (lower panels). Yellow signals in merged panels indicate antigen co-localization. Bar = 20 µm. **d** Western blot analysis of recombinant CD34•IgG-FLAG and MAdCAM-1•IgG-FLAG proteins decorated with 297-11A-positive sulfated glycans. Membrane was immunoblotted (IB'd) with anti-FLAG M2 (left panel) or 297-11A (right panel)

differ stereochemically: Gal and Fuc residues are attached to GlcNAc in β1,4- and β1,3-linkages, respectively, in sialyl Le^X (type 2 chain) and in the reverse positions in sialyl Le^a (type 1 chain) [42]. Considering that 297-11A also binds to 6-sulfo GalNAc attached to GlcNAc in a β1,4-linkage, it is plausible that the 297-11A recognition determinant likely requires (i) 6-*O*-sulfated terminal Gal (indifferent to 2-acetamidation) and (ii) penultimate GlcNAc, regardless of their linking mode (either in β1,4 or β1,3 linkages).

In addition to recognizing 6′-sulfo LacNAc structures, 297-11A also reacts with 6,6′-disulfo LacNAc, and our immunohistochemical studies revealed that a proportion of HEVs in human LNs, particularly those in PLNs, are 297-11A-positive. KSGal6ST and GlcNAc6STs reportedly do not compete for the same acceptor due to their substrate specificities [16]. Moreover, Gal-6-*O*-sulfation by KSGal6ST is reportedly facilitated by 6-sulfate in the penultimate GlcNAc [15, 16]. Furthermore, Patnode et al. [21] demonstrated that *O*-glycans containing sialyl 6,6′-disulfo LacNAc structures were expressed on HEVs in mouse LNs. These observations combined strongly suggest that sialyl 6,6′-disulfo LacNAc-capped *O*-glycans are expressed on HEVs in human LNs as well.

Mitsuoka et al. [32] previously demonstrated that sialyl 6-sulfo Le^X was the major carbohydrate capping structure of L-selectin ligands expressed on HEVs in humans. They concluded that expression of sialyl 6,6′-disulfo Le^X on HEVs was negligible since their antibodies directed against sialyl 6,6′-disulfo Le^X (clones G270-6, G270-11, G270-37, and G270-39) did not react with HEVs [32]. However, this result does not necessarily indicate the absence of sialyl 6,6′-disulfo LacNAc structures, as those anti-sialyl 6,6′-disulfo Le^X antibodies may require GlcNAc-α1,3-fucosylation for the epitope and thus not react with sialyl 6,6′-

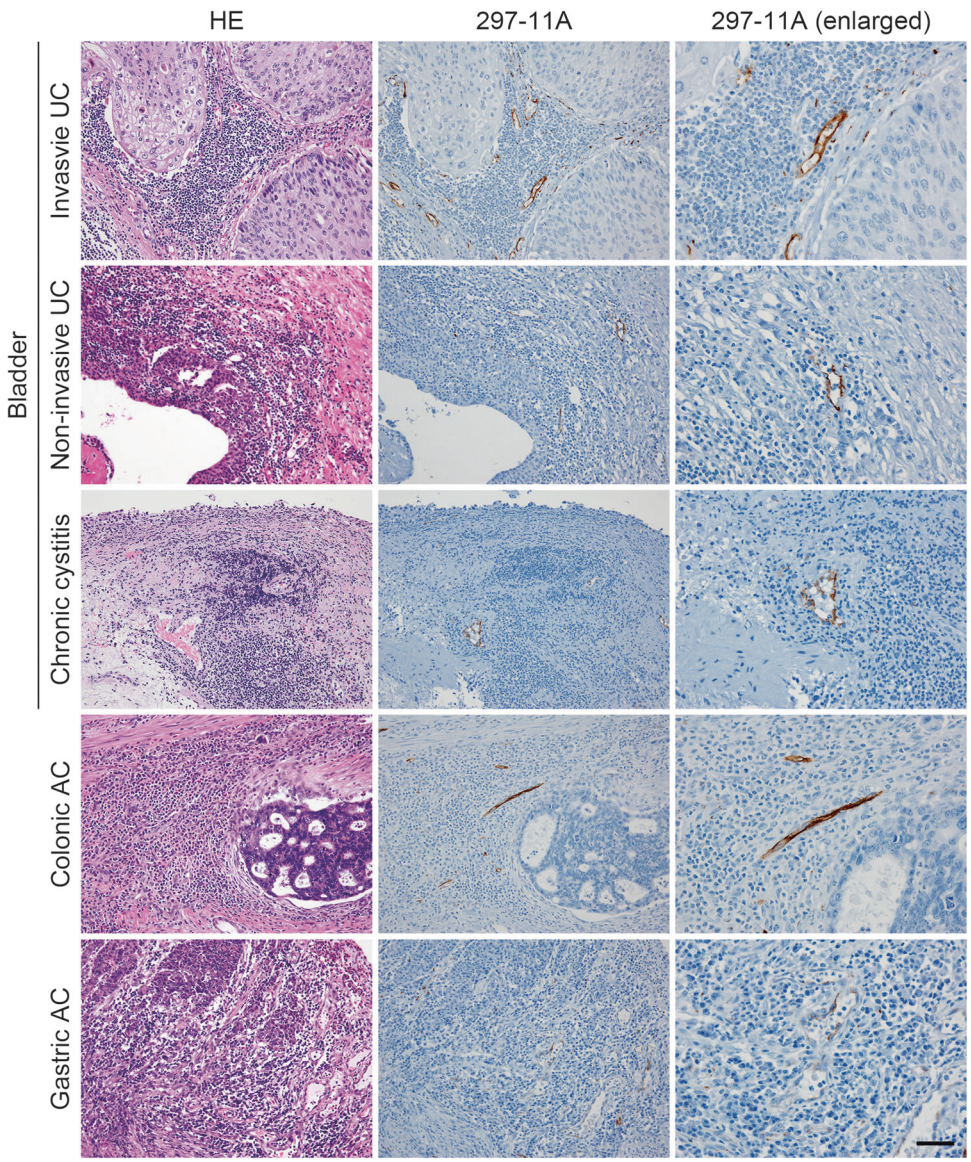

Fig. 10 Expression of 297-11A sulfated glycans on high endothelial venule (HEV)-like vessels induced in tumor-infiltrating lymphocyte (TIL) aggregates formed in indicated cancers and in chronic cystitis. Serial tissue sections were stained with hematoxylin and eosin (HE) and, after HCl treatment, immunostained for 297-11A. Images at right are enlarged from those in middle panels. Signals were visualized with 3,3′-diaminobenzidine (brown), and tissues were counterstained with hematoxylin. UC urothelial carcinoma, AC adenocarcinoma. Bar = 80 μm for left and middle panels and 40 μm for right panels

disulfo LacNAc potentially expressed on HEVs in human LNs.

In our analysis of human tissues, the percentage of HEVs displaying sialyl 6′-sulfo (and/or 6,6′-disulfo) LacNAc-capped *O*-glycans was 18.0% and 7.0% in PLNs and MLNs, respectively (see Fig. 8f), while in mice, nearly all HEVs in PLNs and MLNs reportedly react with the monoclonal antibody G270-2, which recognizes sialyl 6,6′-disulfo LacNAc [21]. This discrepancy with our findings might be due to species differences. Alternatively, G270-2 may also recognize 6-sulfo Gal-containing structures other than sialyl 6,6′-disulfo LacNAc.

We demonstrate here that most 297-11A-positive HEVs are also PNAd-positive based on MECA-79 or HECA-452 staining. Given the carbohydrate epitopes recognized by these antibodies (see Fig. 2), endothelial cells found in HEVs likely express a battery of glycosyltransferases and sulfotransferases potentially capable of elaborating sialyl 6,6′-disulfo Le^X-capped *O*-glycans. However, since Gal-6-*O*-sulfation and GlcNAc-α1,3-fucosylation within the same LacNAc unit is mutually exclusive in vivo [11, 14–16], we conclude that endothelial cells found in HEVs do not synthesize sialyl 6,6′-disulfo Le^X but rather express a mixture of sialyl 6-sulfo Le^X and sialyl 6′-sulfo (and/or 6,6′-disulfo) LacNAc.

We also found that 56.9% and 36.8% of vessels in PLNs and MLNs, respectively, were MECA-79-positive, while HECA-452-positive HEVs constituted 38.7% and 25.4% in PLNs and MLNs, respectively. Given that HEVs display fully glycosylated and sulfated forms of L-selectin ligands such as sialyl 6-sulfo Le^X attached to both extended core 1 and core 2-branched *O*-glycans, the percentage of HECA-

452-positive and MECA-79-positive vessels should be comparable. Thus, carbohydrate structures displayed on the MECA-79-positive/HECA-452-negative HEVs, which constitute 18.2% and 11.4% of vessels in PLNs and MLNs, respectively, likely lack GlcNAc-α1,3-fucosylation, such as sialyl 6,6′-disulfo LacNAc, as Gal-6-*O*-sulfation competes with GlcNAc-α1,3-fucosylation in the same LacNAc side chain [11, 14–16]. Accordingly, we found the percentage of HEVs expressing sialyl 6′-sulfo (and/or 6,6′-disulfo) LacNAc-capped *O*-glycan in PLNs and MLNs to be 18.0% and 7.0%, respectively (see Fig. 8f).

Our study reveals that sialyl 6′-sulfo (and/or 6,6′-disulfo) LacNAc-capped *O*-glycans are preferentially displayed on HEVs in PLNs, and to a lesser extent on those in MLNs, but not in PPs. The fact that the scaffold protein MAdCAM-1 is exclusively expressed on HEVs in PPs and MLNs but not in PLNs [7, 8], may partially explain this finding, as our western blot analysis demonstrated that MAdCAM-1 proteins were less efficiently decorated with 297-11A-positive sulfated glycans than were CD34 proteins. We previously demonstrated that the sulfotransferase GlcNAc6ST-1 prefers acceptor substrates on MAdCAM-1 proteins rather than those on CD34 proteins [35]. We speculate that, conversely, KSGal6ST may favor acceptor substrates on CD34 rather than MAdCAM-1 proteins, although mechanisms remain to be elucidated. Alternatively, the number of potential *O*-glycosylation sites on these two scaffold proteins (79 and 57 sites on CD34 and MAdCAM-1, respectively) may affect the overall presentation of sialyl 6′-sulfo (and/or 6,6′-disulfo) LacNAc-capped *O*-glycans on HEVs in PLNs and MLNs [5–8]. Further studies are required to clarify these issues.

In the present study, we also demonstrate that 297-11A-positive sulfated glycans are displayed on HEV-like vessels induced in TIL aggregates formed in cancers such as bladder urothelial carcinoma and colonic and gastric adenocarcinomas, suggesting a potential role of these sulfated glycans in TIL recruitment in multiple contexts. Also under chronic inflammatory conditions, vessels morphologically analogous to HEVs are induced in non-lymphoid tissues, and these HEV-like vessels are implicated in pathologic lymphocyte recruitment from the circulation to the site of inflammation [4, 43]. In the present study, while we demonstrate induction of 297-11A-positive HEV-like vessels in chronic cystitis, a chronic inflammatory condition of bladder, we previously demonstrated induction of PNAd-expressing HEV-like vessels in chronic inflammatory conditions, including chronic *Helicobacter pylori* gastritis [24, 29, 30], ulcerative colitis [35, 44], autoimmune pancreatitis [45], chronic prostatitis associated with benign prostatic hyperplasia [46] and, most recently, eosinophilic chronic rhinosinusitis (ECRS) [27]. It is of great interest to determine whether sialyl 6′-sulfo (and/or 6,6′-disulfo) LacNAc-capped *O*-glycans are also expressed on these vessels. As GlcNAc-α1,3-fucosylation, which represents a pivotal step in biosynthesis of PNAd carbohydrates and is crucial for recognition by L-selectin, is inhibited by KSGal6ST-mediated Gal-6-*O*-sulfation [11, 14–16], it is tempting to speculate that KSGal6ST may negatively regulate L-selectin-dependent lymphocyte recruitment and of consequent chronic inflammation. Another possibility is that sialyl 6′-sulfo (and/or 6,6′-disulfo) LacNAc-capped *O*-glycans potentially expressed on HEV-like vessels may contribute to Siglec-8-mediated eosinophil recruitment in allergic inflammation such as ECRS.

In addition to HEVs and HEV-like vessels, expression of MECA-79 sulfated glycans has also been reported in some tumor types [38, 41, 47, 48]. Among these studies, Okayama et al. [47] reported that MECA-79 glycoepitopes were aberrantly expressed in ~25% of gastric adenocarcinoma, and such expression was correlated with depth of invasion, venous invasion, disease stage, distant metastasis, and worse prognosis. On the other hand, we previously reported that MECA-79 sulfated glycans are preferentially expressed at the apical membrane of cholangiocytes found in canalicular structures formed in cholangiolocellular carcinoma (CoCC), a finding that could identify a useful CoCC marker [38]. Similarly, if a particular tumor type, or the histological architecture of that tumor type, preferentially expresses 297-11A-positive sulfated glycans, the monoclonal antibody 297-11A should be a valuable tool for the diagnosis of that tumor.

Acknowledgements We thank Noriko Maruta, Hisataka Kato, Shinichi Fujii, and Moriyasu Hattori for technical assistance, Masaru Inatani for providing porcine corneal tissue used for a positive control of 5D4 immunostaining, Kenji Uchimura, Kay-Hooi Khoo, and Tsutomu Katsuyama for useful discussion, and Elise Lamar for critical reading of the manuscript. We also thank the Non-Profit Organization for Biotechnology Research and Development, Osaka, Japan for technical assistance with *Chst1* KO mouse re-derivation. The *Chst1* KO mouse strain used here was generated by the trans-NIH Knock-Out Mouse Project (KOMP) and obtained from the KOMP Repository (www.comp.org), which was supported by NIH grants U01HG004085 (to Velocigene at Regeneron, Inc), U01HG004080 (to the CSD Consortium) and U42RR024244 (to the KOMP Repository at UC Davis and CHORI). For more information or to obtain KOMP products go to www.komp.org or email service@komp.org. This work was supported by Grants-in-Aid for Scientific Research 17K08758 (to HH), 16K15739 (to TOA) and 15K08343 (to MK) from the Japan Society for the Promotion of Science. Part of the work was presented as a poster at the San Diego Glycobiology Symposium, held in San Diego, CA, February 1–2, 2019.

Compliance with ethical standards

Conflict of interest The authors declare that they have no conflict of interest.

References

1. Kobayashi M, Hoshino H, Suzawa K, Sakai Y, Nakayama J, Fukuda M. Two distinct lymphocyte homing systems involved in the pathogenesis of chronic inflammatory gastrointestinal diseases. Semin Immunopathol. 2012;34:401–13.
2. Rosen SD. Ligands for L-selectin: homing, inflammation, and beyond. Annu Rev Immunol. 2004;22:129–56.
3. Butcher EC, Picker LJ. Lymphocyte homing and homeostasis. Science. 1996;272:60–6.
4. Sakai Y, Kobayashi M. Lymphocyte 'homing' and chronic inflammation. Pathol Int. 2015;65:344–54.
5. Puri KD, Finger EB, Gaudernack G, Springer TA. Sialomucin CD34 is the major L-selectin ligand in human tonsil high endothelial venules. J Cell Biol. 1995;131:261–70.
6. Hernandez Mir G, Helin J, Skarp KP, Cummings RD, Mäkitie A, Renkonen R, et al. Glycoforms of human endothelial CD34 that bind L-selectin carry sulfated sialyl Lewis X capped *O*- and *N*-glycans. Blood. 2009;114:733–41.
7. Berg EL, McEvoy LM, Berlin C, Bargatze RF, Butcher EC. L-selectin-mediated lymphocyte rolling on MAdCAM-1. Nature. 1993;366:695–8.
8. Shyjan AM, Bertagnolli M, Kenney CJ, Briskin MJ. Human mucosal addressin cell adhesion molecule-1 (MAdCAM-1) demonstrates structural and functional similarities to the α4β7-integrin binding domains of murine MAdCAM-1, but extreme divergence of mucin-like sequences. J Immunol. 1996;156:2851–7.
9. Streeter PR, Rouse BT, Butcher EC. Immunohistologic and functional characterization of a vascular addressin involved in lymphocyte homing into peripheral lymph nodes. J Cell Biol. 1988;107:1853–62.
10. Yeh JC, Hiraoka N, Petryniak B, Nakayama J, Ellies LG, Rabuka D, et al. Novel sulfated lymphocyte homing receptors and their control by a core 1 extension β1,3-*N*-acetylglucosaminyltransferase. Cell. 2001;105:957–69.
11. Homeister JW, Thall AD, Petryniak B, Malý P, Rogers CE, Smith PL, et al. The α(1,3)fucosyltransferases FucT-IV and FucT-VII exert collaborative control over selectin-dependent leukocyte recruitment and lymphocyte homing. Immunity. 2001;15:115–26.
12. Hemmerich S, Rosen SD. 6′-Sulfated sialyl Lewis X is a major capping group of GlyCAM-1. Biochemistry. 1994;33:4830–5.
13. Hemmerich S, Leffler H, Rosen SD. Structure of the *O*-glycans in GlyCAM-1, an endothelial-derived ligand for L-selectin. J Biol Chem. 1995;270:12035–47.
14. Malý P, Thall A, Petryniak B, Rogers CE, Smith PL, Marks RM, et al. The α(1,3)fucosyltransferase Fuc-TVII controls leukocyte trafficking through an essential role in L-, E-, and P-selectin ligand biosynthesis. Cell. 1996;86:643–53.
15. Torii T, Fukuta M, Habuchi O. Sulfation of sialyl *N*-acetyllactosamine oligosaccharides and fetuin oligosaccharides by keratan sulfate Gal-6-sulfotransferase. Glycobiology. 2000;10:203–11.
16. Hiraoka N, Petryniak B, Kawashima H, Mitoma J, Akama TO, Fukuda MN, et al. Significant decrease in α1,3-linked fucose in association with increase in 6-sulfated *N*-acetylglucosamine in peripheral lymph node addressin of FucT-VII-deficient mice exhibiting diminished lymphocyte homing. Glycobiology. 2007;17:277–93.
17. Kawashima H, Petryniak B, Hiraoka N, Mitoma J, Huckaby V, Nakayama J, et al. *N*-acetylglucosamine-6-*O*-sulfotransferases 1 and 2 cooperatively control lymphocyte homing through L-selectin ligand biosynthesis in high endothelial venules. Nat Immunol. 2005;6:1096–104.
18. Uchimura K, Gauguet JM, Singer MS, Tsay D, Kannagi R, Muramatsu T, et al. A major class of L-selectin ligands is eliminated in mice deficient in two sulfotransferases expressed in high endothelial venules. Nat Immunol. 2005;6:1105–13.
19. Kitayama K, Hayashida Y, Nishida K, Akama TO. Enzymes responsible for synthesis of corneal keratan sulfate glycosaminoglycans. J Biol Chem. 2007;282:30085–96.
20. Bistrup A, Bhakta S, Lee JK, Belov YY, Gunn MD, Zuo FR, et al. Sulfotransferases of two specificities function in the reconstitution of high endothelial cell ligands for L-selectin. J Cell Biol. 1999;145:899–910.
21. Patnode ML, Yu SY, Cheng CW, Ho MY, Tegesjö L, Sakuma K, et al. KSGal6ST generates galactose-6-*O*-sulfate in high endothelial venules but does not contribute to L-selectin-dependent lymphocyte homing. Glycobiology. 2013;23:381–94.
22. Hayashida Y, Akama TO, Beecher N, Lewis P, Young RD, Meek KM, et al. Matrix morphogenesis in cornea is mediated by the modification of keratan sulfate by GlcNAc 6-*O*-sulfotransferase. Proc Natl Acad Sci USA. 2006;103:13333–8.
23. Hirakawa J, Tsuboi K, Sato K, Kobayashi M, Watanabe S, Takakura A, et al. Novel anti-carbohydrate antibodies reveal the cooperative function of sulfated *N*- and *O*-glycans in lymphocyte homing. J Biol Chem. 2010;285:40864–78.
24. Kobayashi M, Mitoma J, Nakamura N, Katsuyama T, Nakayama J, Fukuda M. Induction of peripheral lymph node addressin in human gastric mucosa infected by *Helicobacter pylori*. Proc Natl Acad Sci USA. 2004;101:17807–12.
25. Kikly KK, Bochner BS, Freeman SD, Tan KB, Gallagher KT, D'alessio KJ, et al. Identification of SAF-2, a novel Siglec expressed on eosinophils, mast cells, and basophils. J Allergy Clin Immunol. 2000;105:1093–100.
26. Floyd H, Ni J, Cornish AL, Zeng Z, Liu D, Carter KC, et al. Siglec-8. A novel eosinophil-specific member of the immunoglobulin superfamily. J Biol Chem. 2000;275:861–6.
27. Tsutsumiuchi T, Hoshino H, Fujieda S, Kobayashi M. Induction of peripheral lymph node addressin in human nasal mucosa with eosinophilic chronic rhinosinusitis. Pathology. 2019;51:268–73.
28. Hao P, Ren Y, Xie Y. An improved protocol for *N*-glycosylation analysis of gel-separated sialylated glycoproteins by MALDI-TOF/TOF. PLoS ONE. 2010;5:e15096.
29. Kobayashi M, Mitoma J, Hoshino H, Yu SY, Shimojo Y, Suzawa K, et al. Prominent expression of sialyl Lewis X-capped core 2-branched *O*-glycans on high endothelial venule-like vessels in gastric MALT lymphoma. J Pathol. 2011;224:67–77.
30. Okamura T, Sakai Y, Hoshino H, Iwaya Y, Tanaka E, Kobayashi M. Superficially located enlarged lymphoid follicles characterise nodular gastritis. Pathology. 2015;47:38–44.
31. Duijvestijn AM, Horst E, Pals ST, Rouse BN, Steere AC, Picker LJ, et al. High endothelial differentiation in human lymphoid and inflammatory tissues defined by monoclonal antibody HECA-452. Am J Pathol. 1988;130:147–55.
32. Mitsuoka C, Sawada-Kasugai M, Ando-Furui K, Izawa M, Nakanishi H, Nakamura S, et al. Identification of a major carbohydrate capping group of the L-selectin ligand on high endothelial venules in human lymph nodes as 6-sulfo sialyl Lewis X. J Biol Chem. 1998;273:11225–33.
33. Hoshino H, Foyez T, Ohtake-Niimi S, Takeda-Uchimura Y, Michikawa M, Kadomatsu K, et al. KSGal6ST is essential for the 6-sulfation of galactose within keratan sulfate in early postnatal brain. J Histochem Cytochem. 2014;62:145–56.
34. Fujiwara M, Kobayashi M, Hoshino H, Uchimura K, Nakada T, Masumoto J, et al. Expression of long-form *N*-acetylglucosamine-6-*O*-sulfotransferase 1 in human high endothelial venules. J Histochem Cytochem. 2012;60:397–407.
35. Kobayashi M, Hoshino H, Masumoto J, Fukushima M, Suzawa K, Kageyama S, et al. GlcNAc6ST-1-mediated decoration of MAdCAM-1 protein with L-selectin ligand carbohydrates directs

disease activity of ulcerative colitis. Inflamm Bowel Dis. 2009;15:697–706.
36. Hoshino H, Kobayashi M, Mitoma J, Sato Y, Fukuda M, Nakayama J. An integrin α4β7•IgG heterodimeric chimera binds to MAdCAM-1 on high endothelial venules in gut-associated lymphoid tissue. J Histochem Cytochem. 2011;59:572–83.
37. Akama TO, Nakayama J, Nishida K, Hiraoka N, Suzuki M, McAuliffe J, et al. Human corneal GlcNAc 6-*O*-sulfotransferase and mouse intestinal GlcNAc 6-*O*-sulfotransferase both produce keratan sulfate. J Biol Chem. 2001;276:16271–8.
38. Hoshino H, Ohta M, Ito M, Uchimura K, Sakai Y, Uehara T, et al. Apical membrane expression of distinct sulfated glycans represents a novel marker of cholangiolocellular carcinoma. Lab Invest. 2016;96:1246–55.
39. Kiwamoto T, Brummet ME, Wu F, Motari MG, Smith DF, Schnaar RL, et al. Mice deficient in the St3gal3 gene product α2,3 sialyltransferase (ST3Gal-III) exhibit enhanced allergic eosinophilic airway inflammation. J Allergy Clin Immunol. 2014;133:240–7.e1–3.
40. Pröpster JM, Yang F, Rabbani S, Ernst B, Allain FH, Schubert M. Structural basis for sulfation-dependent self-glycan recognition by the human immune-inhibitory receptor Siglec-8. Proc Natl Acad Sci USA. 2016;113:E4170–9.
41. Taga M, Hoshino H, Low S, Imamura Y, Ito H, Yokoyama O, et al. A potential role for 6-sulfo sialyl Lewis X in metastasis of bladder urothelial carcinoma. Urol Oncol. 2015;33:496.e1–9.
42. Berg EL, Robinson MK, Mansson O, Butcher EC, Magnani JL. A carbohydrate domain common to both sialyl Le^a and sialyl Le^X is recognized by the endothelial cell leukocyte adhesion molecule ELAM-1. J Biol Chem. 1991;266:14869–72.
43. Aloisi F, Pujol-Borrell R. Lymphoid neogenesis in chronic inflammatory diseases. Nat Rev Immunol. 2006;6:205–17.
44. Suzawa K, Kobayashi M, Sakai Y, Hoshino H, Watanabe M, Harada O, et al. Preferential induction of peripheral lymph node addressin on high endothelial venule-like vessels in the active phase of ulcerative colitis. Am J Gastroenterol. 2007;102:1499–509.
45. Maruyama M, Kobayashi M, Sakai Y, Hiraoka N, Ohya A, Kageyama S, et al. Periductal induction of high endothelial venule-like vessels in type 1 autoimmune pancreatitis. Pancreas. 2013;42:53–9.
46. Inamura S, Shinagawa T, Hoshino H, Sakai Y, Imamura Y, Yokoyama O, et al. Appearance of high endothelial venule-like vessels in benign prostatic hyperplasia is associated with lower urinary tract symptoms. Prostate. 2017;77:794–802.
47. Okayama H, Kumamoto K, Saitou K, Hayase S, Kofunato Y, Sato Y, et al. Ectopic expression of MECA-79 as a novel prognostic indicator in gastric cancer. Cancer Sci. 2011;102:1088–94.
48. Yu SY, Hsiao CT, Izawa M, Yusa A, Ishida H, Nakamura S, et al. Distinct substrate specificities of human GlcNAc-6-sulfotransferases revealed by mass spectrometry-based sulfoglycomic analysis. J Biol Chem. 2018;293:15163–77.